Structural Characterization of Lipoarabinomannans from *Mycobacterium tuberculosis* and *Mycobacterium smegmatis* by ESI Mass Spectrometry

Christopher J. Petzold, Leslie H. Stanton, and Julie A. Leary
Genome Center, Department of Chemistry and Molecular Cell Biology, University of California at Davis, Davis, California, USA

Structural aspects of lipoarabinomannans (LAM) from *Mycobacterium tuberculosis* and *Mycobacterium smegmatis* were investigated by using mild acid hydrolysis in combination with Fourier-transform ion cyclotron resonance (FT-ICR), and quadrupole ion trap mass spectrometry. Exact mass measurements with less than 2.5 ppm mass error confirmed the presence of a series of arabinose oligomers (Ara_n; n = 2–7) as the major components observed following mild acid hydrolysis of both *M. tuberculosis* and *M. smegmatis* LAM. However, the mass spectrum of the resulting LAM extract also revealed a highly-abundant distribution of ions that exact mass measurements identified as mannose-linked arabinose species, $Ara_nMan_m + Na^+$ (n = 1–6; m = 1–3). The observed mannose caps were linked to arabinose species as mono-, di-, and trimannose units, and the ratio of the mono-, di-, and trimannose caps was determined to be 1.00:9.00:1.15, respectively, different from previous reports. Analysis of the linkage of lithiated arabinose trimer standards was accomplished with MS^3 experiments and the information generated was used to identify linkages of arabinose trimers generated by mild acid hydrolysis of *M. tuberculosis* and *M. smegmatis* LAM. The MS^3 spectra confirmed the linkage of arabinose trimers from *M. smegmatis* and *M. tuberculosis* LAM as predominantly $\alpha(1 \rightarrow 5)$, $\alpha(1 \rightarrow 5)$. (J Am Soc Mass Spectrom 2005, 16, 1109-1116) © 2005 American Society for Mass Spectrometry

Tuberculosis is a serious worldwide problem that causes approximately 8 million new active cases and 2–3 million deaths each year [1]. Indeed, approximately one third of the population of the world is infected by *M. tuberculosis*, however less than 10% of them will develop the active disease [1]. Despite the use of a wide variety of antibiotics, tuberculosis has re-emerged as a health problem in industrialized countries mainly due to persistence of drug-resistant strains. Consequently, the factors that lead to the survival of *M. tuberculosis* in the host are active areas of research. The complex relationship between the host defense mechanisms and the molecular means by which *M. tuberculosis* circumvents them is particularly interesting.

The unique cell wall of *M. tuberculosis* forms a waxy envelope and has been established as an important factor leading to bacterial virulence and survival [2]. As a consequence, effective antibiotics often target the biosynthetic pathways that lead to formation of components of the cell wall. The cell wall of *M. tuberculosis* and related mycobacteria consists of a variety of lipoglycans (lipoarabinomannans, phosphatidyl-*myo*-inositol mannosides, and lipomannans), long-chain fatty acids (mycolic acids) and polysaccharides [2, 3]. One of the principle components of the cell wall of mycobacteria is the lipoarabinomannan (LAM). LAM are complex, highly heterogeneous lipoglycans that are characterized by three main components: a mannosylphosphatidyl-*myo*-inositol linker, a polysaccharide backbone that consists of a mannan backbone and branched arabinan chains, and a capping motif (Figure 1) [4]. The mannan portion is a linear chain of $\alpha 1 \rightarrow$ 6-D-Man*p* residues to which individual $\alpha 1 \rightarrow$ 2-D-Man*p* units are linked. The arabinan chains are comprised of $\alpha 1 \rightarrow$ 5-D-Ara*f* repeats punctuated with $\alpha 1 \rightarrow$ 3-D-Ara*f* branches organized as either linear tetra-arabinofuranosides (β-D-Ara*f*-(1 $\rightarrow$ 2)-α-D-Ara*f*-(1 $\rightarrow$ 5)-α-D-Ara*f*-(1 $\rightarrow$ 5)-α-D-Ara*f*) or as branched hexa-arabinofuranosides ([β-D-Ara*f*-(1 $\rightarrow$ 2)-α-D-Ara*f*-(1-]$_2$ $\rightarrow$ 3, and $\rightarrow$ 5)-α-D-Ara*f*-(1 $\rightarrow$ 5)-α-D-Ara*f*) [4, 5]. The extent of arabinan branching is known from methylation analysis, however, the location of the branches and even the number of arabinan chains connected to the mannan backbone have yet to be determined. The most variable portion of LAM is the capping motif. *M. leprae, M. bovis*, and several strains of *M. tuberculosis* (Erdman, H37Rv, H37Ra) contain mannose caps (ManLAM) while fast growing *M. smegmatis*

Published online May 31, 2005

Address reprint requests to Professor J. A. Leary, Department of Chemistry and Molecular Cell Biology, Genome Center, University of California at Davis, One Shields Road, Davis, CA 95616, USA. E-mail: jaleary@ucdavis.edu

1044-0305/05/$30.00
doi:10.1016/j.jasms.2005.02.023

Received November 29, 2004
Revised February 17, 2005
Accepted February 23, 2005

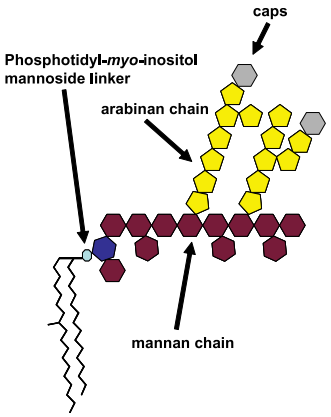

Figure 1. Structural representation of LAM.

has phosphatidyl-*myo*-inositol caps (PILAM) [5]. Recently, a LAM devoid of caps was discovered in *M. chelonae*, and a unique capping structure, 5-deoxy-5-methyl-thio-pentofuranose, has been observed in low abundance in *M. tuberculosis* LAM [6].

While information is available concerning the basic composition of LAM from various mycobacteria, there is a significant need to obtain more specific structural information and to correlate the complete fine structure of the LAM with their biological functions. The immunological properties of LAM from both virulent and avirulent species have been studied [7–12], and it is becoming increasingly apparent that subtle differences in LAM structure may shape the host response to various species. For instance, mannose-capped LAM from *M. tuberculosis* causes apoptosis inhibition and suppresses TNF-α and IL-12 production, while PILAM from *M. smegmatis* invoke entirely opposite macrophage functions [8, 12]. ManLAM, unlike PILAM, have been shown to bind to the mannose receptor [13] which aids in macrophage phagocytosis [11]. Binding of human pulmonary surfactant protein A to *M. bovis* BCG LAM is dependent on the presence of both mannose caps and the phosphatidyl-*myo*-inositol linker [14]. Likewise, *M. leprae* LAM devoid of their phosphatidyl-*myo*-inositol anchor are unable to stimulate T-cell responses, suggesting that structural aspects of the linker are important to the recognition of the carbohydrate epitopes [15].

Initial characterization of the linkage and carbohydrate composition of lipoarabinomannans have been obtained via mild acid hydrolysis, methylation of the hydroxyl groups, and HPLC purification before analysis by mass spectrometry and NMR experiments [16]. However, such procedures often require a large amount of LAM and as a consequence, recent structural studies of mild acid hydrolyzed LAM have been conducted using off-line capillary electrophoresis with laser-induced fluorescence and subsequent MALDI [17] or ESI [18] mass spectrometry. Although the amount of LAM used in these experiments is greatly decreased, the degraded LAM must be derivatized with a suitable chromophore to enable detection by LIF. In our laboratory, a variety of methods have been developed to differentiate linkage position, stereochemistry and general topology of carbohydrates by mass spectrometry [19–23]. In this report, we utilize mild acid hydrolysis, Fourier-transform ion cyclotron resonance (FT-ICR), and quadrupole ion trap mass spectrometry coupled with multiple stages of collision-induced dissociation (CID) to analyze the structure of lipoarabinomannans isolated from *M. smegmatis* and *M. tuberculosis*. Using FT-ICR mass spectrometry and exact mass measurements, a series of arabinose oligomers were identified from both *M. smegmatis* and *M. tuberculosis*, and mannose caps are observed in the spectra of the *M. tuberculosis* LAM. Alkali metal coordination followed by CID was used to differentiate between the linkages of arabinan standards and was subsequently used to obtain specific linkage information of LAM isolated from *M. smegmatis* and *M. tuberculosis*.

Experimental

Chemicals

All chemicals and solvents, except chloroform and methanol (Fisher, Fairborn, NJ), were obtained from Sigma Chemical Co. (St. Louis, MO) and were used without further purification unless otherwise specified. All solvents were of HPLC grade. Purified water was generated with a Milli-Q water purification system operating at 18.2 MΩ. Arabinose trimer standards, Ara*f*-(1 $\rightarrow$ 2)-α-D-Ara*f*-(1 $\rightarrow$ 5)α-D-Ara*f* (OMR-3) and Ara*f*-(1 $\rightarrow$ 5)-α-D-Ara*f*-(1 $\rightarrow$ 5)α-D-Ara*f* (TR-2), as well as an arabinose dimer, Ara*f*-(1$\rightarrow$2)-α-D-Ara*f* (OMR-2), were donated by Professor Todd L. Lowary (University of British Columbia).

Cell Culture and Purification

Mycobacterium smegmatis strain mc^{2}155 was grown in Middlebrook 7H9 broth supplemented with 10% ADC

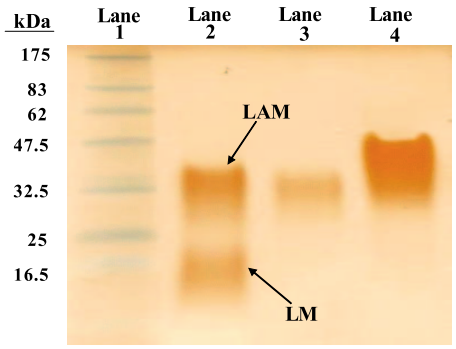

Figure 2. 10–20% Tris-tricine SDS-PAGE analysis of LAM: Lane 1, prestained molecular weight marker. Lane 2, total polysaccharides from *M. smegmatis* before fractionation. Lane 3, fractionated LAM from *M. smegmatis*. Lane 4, pure LAM from *M. tuberculosis*. *M. tuberculosis* LAM is significantly larger than *M. smegmatis* LAM.

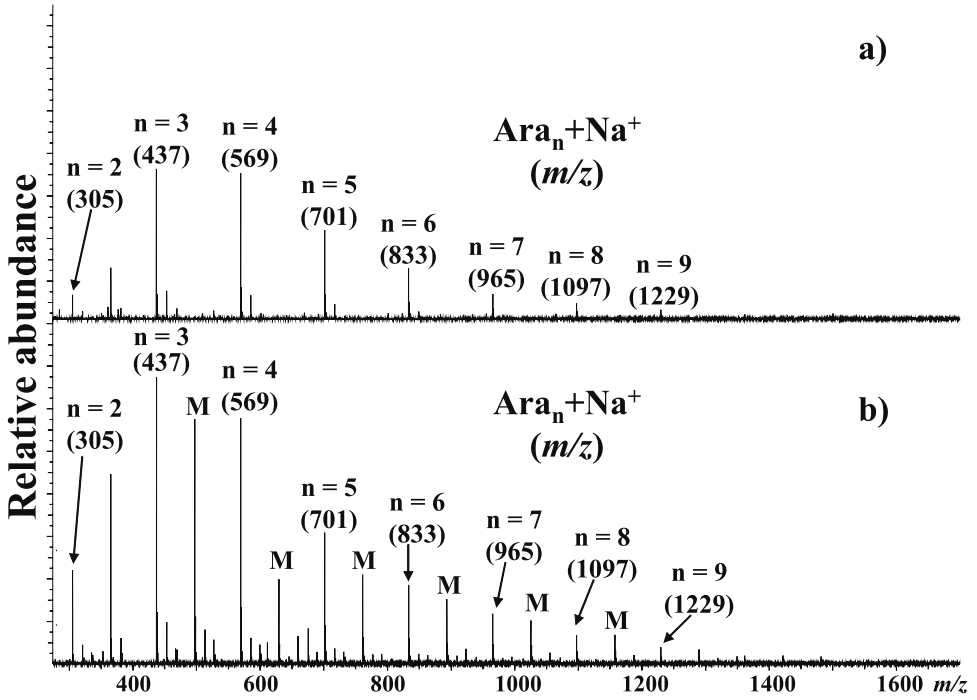

Figure 3. Mass spectra of mild acid hydrolyzed LAM from (**a**) *M. smegmatis* and (**b**) *M. tuberculosis*. A series of Arabinose oligomers (n = number of arabinose units) was observed in both samples. Peaks denoted with an (M) correspond to a series of mannose-arabinose oligomers.

(Difco), 0.05% Tween-80, and 0.2% glycerol. *M. tuberculosis* H37Rv LAM and γ- irradiated cells were obtained from Colorado State University's TB Research Materials and Vaccine Testing contract, NIH NIAID Al-75320. Delipidation of the cells was accomplished by shaking the cells in 2:1 CCl_3H: Methanol at 50 °C for 3 h. The LAM were isolated from delipidated cells in 50% aqueous ethanol followed by evaporation to dryness and subsequent extraction with PBS-saturated phenol. After dialyzing for 2 days, the LAM were lyophilized and further purified by Sephacryl S-200 gel filtration chromatography in a buffer containing 10 mM Tris-HCl pH 8.0, 1 mM EDTA, 0.2 M NaCl, 0.25% sodium deoxycholate, and 0.02% sodium azide. Fractions were visualized by 10–20% tris-tricine gels which were silver stained with the inclusion of a periodate oxidase step. A prestained molecular weight marker (New England Biolabs, Beverly, MA) was included on each gel. LAM-containing fractions were dialyzed against column buffer lacking detergent for 2 days and subsequently dialyzed against water for 3 days.

Table 1. Composition analysis of mild acid hydrolyzed LAM from *M. smegmatis*

Composition	Measured *m/z*	Theoretical *m/z*	Error (ppm)
$Ara_2 + Na^+$	305.0848	305.0843	1.6
$Ara_3 + Na^+$	437.1267	437.1266	0.5
$Ara_4 + Na^+$	569.1687	569.1688	1.2
$Ara_5 + Na^+$	701.2112	701.2111	1.1
$Ara_6 + Na^+$	833.2558	833.2533	0.5

Sample Preparation

Mild acid hydrolysis experiments were performed by incubating LAM in 40 mM trifluoroacetic acid (TFA) at 100 °C for 20 min. The TFA was then removed by drying under a stream of air. The partially degraded LAM was resuspended in 50:50 MeOH:H_2O at a final concentration of 15–30 μM. For CID experiments, alkali metal coordination was accomplished by adding lithium acetate to the sample for a final concentration of 1 mM.

FT-ICR Mass Spectrometry

Exact mass measurements were performed on an Apex II FT-ICR mass spectrometer equipped with a 7T actively shielded superconducting magnet (Bruker Daltonics, Billerica, MA). Sample solutions (15–30 μM in

Table 2. Composition analysis of mild acid hydrolyzed LAM from *M. tuberculosis*

Composition	Measured *m/z*	Theoretical *m/z*	Error (ppm)
$Ara_2 + Na^+$	305.0839	305.0843	1.3
$Ara_3 + Na^+$	437.1263	437.1266	0.6
$Man_2Ara_1 + Na^+$	497.1473	497.1477	0.8
$Ara_4 + Na^+$	569.1692	569.1688	0.7
$Man_2Ara_2 + Na^+$	629.1898	629.1900	0.3
$Ara_5 + Na^+$	701.2122	701.2111	1.5
$Man_2Ara_3 + Na^+$	761.2351	761.2322	1.2
$Ara_6 + Na^+$	833.2515	833.2533	2.1

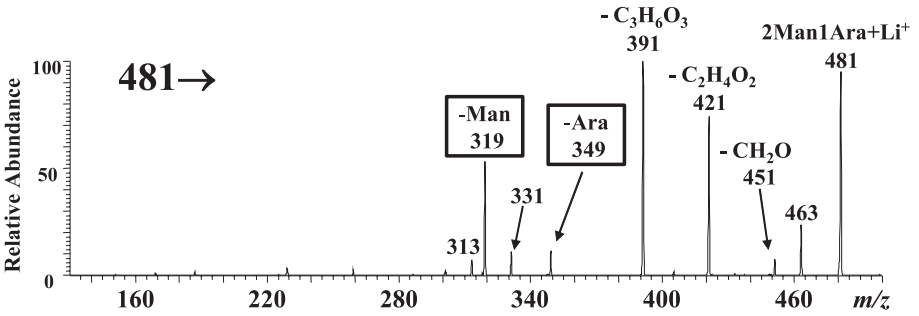

Figure 4. MS^2 mass spectrum of *m/z* 481 from mild acid hydrolyzed TB LAM.

50:50 MeOH:H_2O) were introduced to the ion source via a syringe pump at a flow rate of 2 μL/min. Ions were generated with an Apollo electrospray ionization source (Bruker Daltonics) in positive ion mode. Prior to transfer to the ICR cell, the ions were accumulated for 2 s in a rf-only hexapole. Exact mass measurements were achieved with mannose (MW = 180.0634 Da), OMR-2 (MW = 394.4558 Da), OMR-3 (MW = 526.5701 Da), and isomaltohexose (MW = 990.8564), ionized via sodium cationization as internal calibrants. Each spectrum is composed of 512 k data points (average of 8 scans) and was acquired on the FT-ICR data station, operating Xmass 6.0 (Bruker Daltonics, Madison, WI).

Quadrupole Ion Trap Mass Spectrometry

All CID experiments were carried out on a quadrupole ion trap mass spectrometer (Finnigan LCQ, ThermoFinnigan, San Jose, CA). Sample solutions (15–30 μM in 50:50 MeOH:H_2O) were introduced by direct infusion via a syringe pump at a flow rate of 3–5 μL/min. The capillary was heated to 200 °C and the spray voltage was held at a potential of 5.2 kV. Helium, at a pressure of 1×10^{-3} Torr, was used as both the collision and bath gas. Automatic gain control was utilized to regulate the number of ions in the trap. Spectra are composed of 20 scans of which each scan consists of three "microscans". CID was accomplished using isolation widths of 1 Da and ions were activated at 0.65–0.84 V (normalized collision energy of 25–32%) for 50 ms. For comparative purposes, all arabinose trimers (standards and LAM) were subjected to identical CID conditions.

Results and Discussion

Composition and Capping Motifs

Lipoarabinomannans are highly heterogeneous molecules and the degree of arabinan branching, acylation, and capping are ill-defined. Consequently, the bands visualized on SDS-PAGE (Figure 2) span a wide mass range as seen when compared with the MW markers. Clear separation of the lipomannans (LM) from the LAM can be seen for the sample obtained following extraction with refluxing ethanol (50%) and subsequent extraction with PBS-saturated phenol. Pure LAM is obtained by separation on a Sephacryl S-200 column in detergent. SDS-PAGE reveals that LAM from *M. smegmatis* has a lower average MW than LAM from *M. tuberculosis*, consistent with MALDI-TOF analysis (data not shown). Mild acid hydrolysis of *M. smegmatis* and *M. tuberculosis* LAM was accomplished followed by ESI/FT-ICR mass spectrometry. The mass spectra of the partially hydrolyzed LAM from *M. smegmatis* revealed a distribution of singly-charged ions that differed by 132 Da, the mass of an anhydroarabinose moiety (Figure 3a). The ions observed at *m/z* 305, 421, 569, 701, 833, 965, 1097, and 1229 correspond to sodiated arabinose oligomers ($Ara_n + Na^+$, n = 2–9; Figure 3a). A smaller distribution of potassiated ions are also observed in the spectrum. Exact mass measurements confirmed that the major peaks in the spectrum correspond to $Ara_n + Na^+$ with less than 2.0 ppm error between the measured and calculated masses. A summary of the major ions observed is shown in Table 1. Mild acid hydrolysis experiments conducted with lower concentrations of TFA yielded arabinan chains as large as n = 14.

The $Ara_n + Na^+$ (<1.2 ppm error for n = 2–9; summarized in Table 2) ions are highly abundant in the mild acid hydrolyzed *M. tuberculosis* LAM sample. Unique to the *M. tuberculosis* sample, however, a second highly-abundant distribution of ions (*m/z* 497, 629, 761) is observed. The nominal masses of these ions suggest that they are hexose-linked pentose species, consistent with $Man_mAra_n + Na^+$ (n = 1–6; m = 1–3). Exact mass

Table 3. Mannose caps observed from *M. tuberculosis* LAM after mild acid hydrolysis

Composition[a]	*m/z*	Abundance[b]	Ratio
$Man_1Ara_1 + Na^+$	335	5.45×10^5	
$Man_1Ara_2 + Na^+$	467	7.27×10^5	1.00
$Man_1Ara_3 + Na^+$	599	9.16×10^5	
$Man_2Ara_1 + Na^+$	497	1.15×10^7	
$Man_2Ara_2 + Na^+$	629	3.98×10^6	9.00
$Man_2Ara_3 + Na^+$	761	4.21×10^6	
$Man_3Ara_1 + Na^+$	659	1.33×10^6	
$Man_3Ara_2 + Na^+$	791	4.77×10^5	1.15
$Man_3Ara_3 + Na^+$	923	7.13×10^5	

[a]Only Man_mAra_n ions for n < 4 were used to determine the ratio.
[b]Arbitrary units.

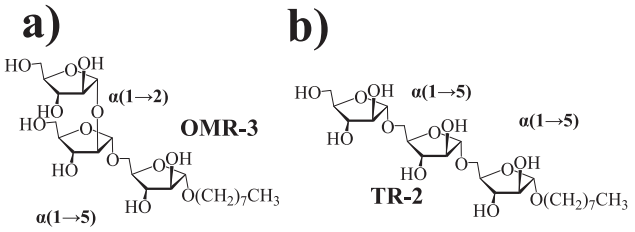

Figure 5. Structure of arabinose trimer standards (**a**) OMR-3 [$\alpha(1 \rightarrow 2),\alpha(1 \rightarrow 5)$ linked] (**b**) TR-2 [$\alpha(1 \rightarrow 5),\alpha(1 \rightarrow 5)$ linked]; both trimers have a saturated eight carbon chain attached at the C1 oxygen.

measurements, with less than 2 ppm error between the theoretical and measured masses, support this identification (Table 2). Under these preparative conditions, preferential cleavages occur in the arabinan domain, suggesting that the Man_mAra_n species are terminal arabinan chains with mannose caps. Only mono-, di-, and trimannose-linked arabinose ions are observed, consistent with previous reports concerning the capping motif of LAM from *M. tuberculosis* [4, 16–18, 24, 25], while LAM isolated from *M. smegmatis* do not contain mannose caps. The mass spectrum obtained following CID of one of the mannose capped species, lithiated Man_2Ara_1 (*m/z* 481), is shown in Figure 4. The loss of 132 Da (*m/z* 349) as well as 162 Da (*m/z* 319) correspond to glycosidic cleavages resulting in the loss of an anhydroarabinose and anhydromannose moiety, respectively. Observance of both species suggests that both moieties are terminal and the Man_2Ara_1 is linked in a linear, not branched, structure.

By summing the abundances (arbitrary units) of the $Ara_nMan_m + Na^+$ ions, we found the ratio of mono-, di-, and trimannose linked caps to be 1.00:9.00:1.15, respectively (Table 3). This is somewhat different from the ratio found by Ludwiczak et al. [17] of 1.1 (±0.1):5.1 (±0.1):0.9 (±0.1) for the mono-, di-, and trimannose units, respectively. The greater abundance of the dimannose caps observed here may be attributed to the inclusion of the di- and triarabinose linked mannose caps that were not included in the previous work, yet under these conditions includes an appreciable amount of Man_2Ara_2 and Man_2Ara_3 species relative to the analogous mono- and trimannose species.

CID and Preliminary Linkage Analysis

It has been shown previously that CID of oligosaccharides that are ionized via alkali metal coordination yields structural information [21, 22, 26–33]. Consequently, characterization of the linkage of the arabinan trimers was accomplished by CID of the mild acid hydrolyzed LAM and comparison to CID observed for arabinose trimer standards of known linkage. Two distinct arabinose trimer standards (Figure 5), OMR-3 (Ara*f*-(1 → 2)-α-D-Ara*f*-(1 → 5)-α-D-Ara*f*) and TR-2 (Ara*f*-(1 → 5)-α-D-Ara*f*-(1 → 5)-α-D-Ara*f*), were ionized via ESI and lithium cationization and subjected to CID. Both standards have a saturated eight-carbon chain at the C1 oxygen of the reducing end. Figure 6 shows the mass spectrum obtained following CID of the lithiated arabinose trimer TR-2. The most abundant product ion in the mass spectrum (*m/z* 401) is identified as a Y_2 ion, per the Domon and Costello nomenclature [34] for fragmentations of oligosaccharides, and corresponds to the loss of the nonreducing end dehydroarabinose moiety. A small amount of *m/z* 269 (Y_1) is observed, but the remaining fragment ions correspond to the charge retained on the nonreducing end, which is quite dissimilar from data collected previously in our laboratory [27, 31, 32]. However, the previously studied lithiated oligomers were devoid of lipid moieties. As can be seen from Figure 6, several ions resulting from the loss of the lipid moiety via cross ring cleavages [*m/z* 361 ($^{0,2}A_3$) and *m/z* 331 ($^{0,3}A_3$)] are observed. Glycosidic cleavages cor-

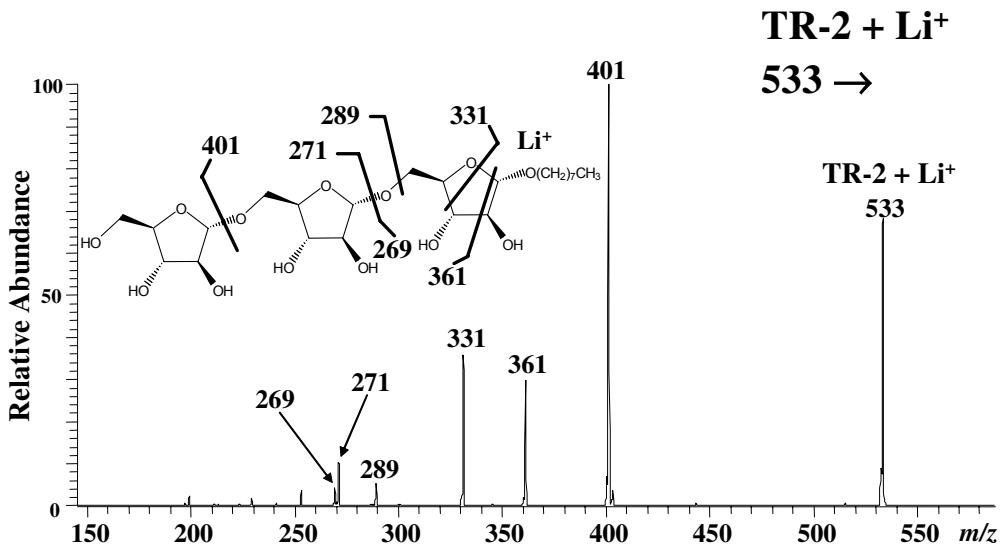

Figure 6. MS^2 specturm of arabinose trimer standard TR-2 (*m/z* 553 →).

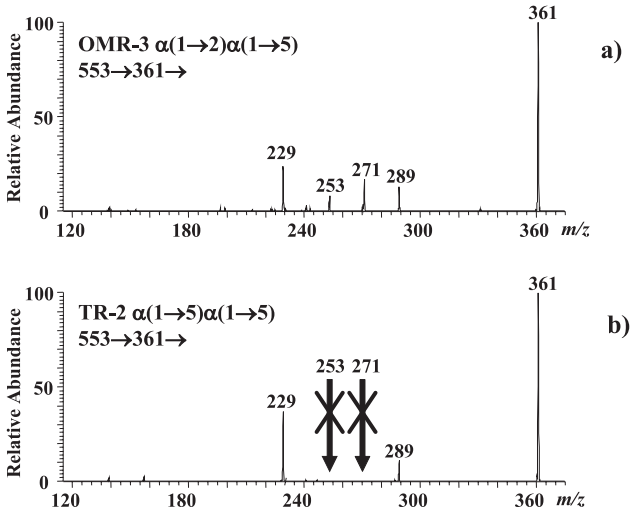

Figure 7. MS^3 spectra (m/z 553 → 361 →) of arabinose trimer standards (**a**) OMR-3 [$\alpha(1 \rightarrow 2),\alpha(1 \rightarrow 5)$ linked] and (**b**) TR-2 [$\alpha(1 \rightarrow 5),\alpha(1 \rightarrow 5)$ linked].

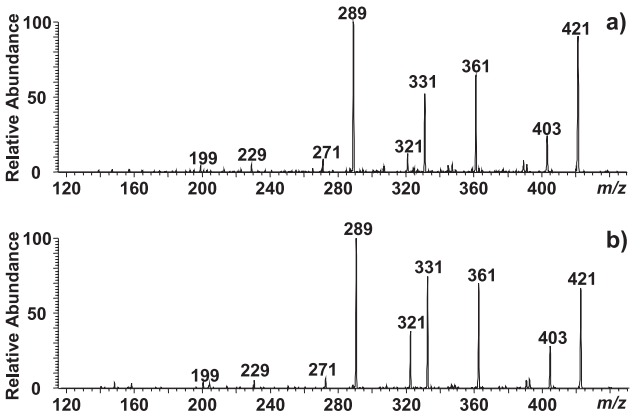

Figure 8. MS^2 spectra (m/z 421 → 361 →) of mild acid hydrolyzed LAM from (**a**) *M. smegmatis* and (**b**) *M. tuberculosis*.

responding to the loss of the arabinose linked at the reducing end [m/z 289 (C_2) and m/z 271 (B_2)] are also detected, however, they are lower in abundance than the previously mentioned cross ring cleavages. Each of these fragment ions, except for the Y_1 ion, retains the distinguishing linkage of the trimer. Thus, it is not surprising that the MS^2 spectra for TR-2 (Figure 6) and OMR-3 (data not shown) are essentially identical, and further stages of CID are necessary to obtain linkage information.

Several of the MS^2 fragment ions (m/z 361, 331, 289) were investigated to determine if diagnostic linkage information could be gathered from MS^3 experiments. In fact, differentiation between the $\alpha(1 \rightarrow 2)$, $\alpha(1 \rightarrow 5)$ and $\alpha(1 \rightarrow 5)$, $\alpha(1 \rightarrow 5)$ linkages is possible with MS^3 for each of the ions investigated, and MS^3 of m/z 361 yields the most distinctly different spectra for the two trimers, which provides diagnostic ions for biological samples. Upon MS^3 of OMR-3, the most abundant fragment ion (m/z 229) corresponds to a loss of 132 Da ($C_5H_8O_4$), (Figure 7a). Several other fragment ions of relatively high abundance are observed at m/z 289, 271, and 253. Fragmentation via the loss of 72 Da yields m/z 289 which corresponds to the C_2 ion formed in the MS^2 experiment discussed above. Subsequent CID on both the MS^2- and MS^3-generated m/z 289 ions yielded identical spectra verifying its identity (data not shown). The ions found at m/z 271 and 253 can be identified as B_2 and $B_2 - H_2O$ species, respectively. Differentiation between the two standards was possible since the m/z 361 ion from the TR-2 trimer (Figure 7b) did not fragment to form either m/z 271 or 253, as seen in the MS^3 of OMR-3. Thus, the presence of m/z 271 (B_2) and m/z 253 ($B_2 - H_2O$) can be used as diagnostic ions to confirm the presence of an $\alpha(1 \rightarrow 2)$, $\alpha(1 \rightarrow 5)$ linkage.

This CID methodology was applied to arabinose trimers generated from the hydrolysis experiment of *M. tuberculosis* and *M. smegmatis* LAM. MS^2 of the lithiated mycobacterial trimers yielded mass spectra (Figure 8) that are essentially identical to each other as well as to the standards. The main difference between the standards and the LAM trimers is the absence of m/z 401 from the CID of the mycobacterial trimers. The absence of this fragment ion is not surprising since it retains the saturated carbon chain on the reducing end arabinose that is unique to the chemically synthesized species. Subjecting the m/z 361 fragment ion from *M. tuberculosis* (Figure 9b) and *M. smegmatis* (Figure 9c) to MS^3 yielded spectra that were most similar to the MS3 spectrum of TR-2 [$\alpha(1 \rightarrow 5)$, $\alpha(1 \rightarrow 5)$]. The *M. tuberculosis* and *M. smegmatis* MS^3 spectra were identical to each other, containing m/z 229, 289, and 271 (very low abundance)

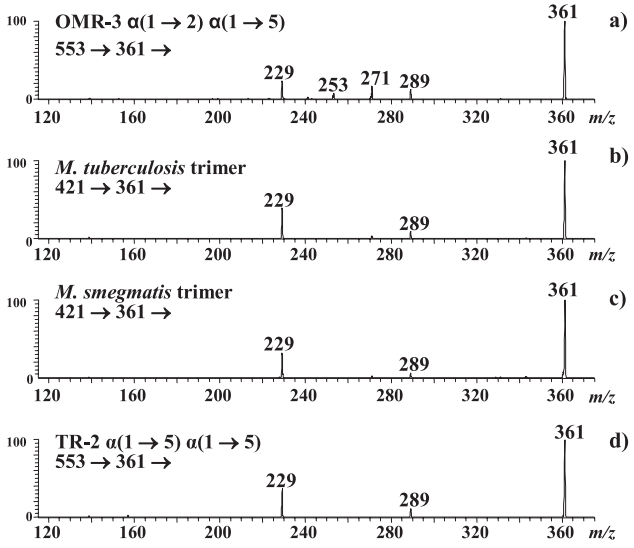

Figure 9. MS^3 spectra (m/z 553 → 361 →) of arabinose trimer standards (**a**) OMR-3 and (**d**) TR-2 and the corresponding mild acid hydrolyzed LAM (m/z 421 → 361 →) from (**b**) *M. tuberculosis* and (**c**) *M. smegmatis*. MS3 spectra of both the LAM trimers are similar to that of TR-2 suggesting that they are $\alpha(1 \rightarrow 5),\alpha(1 \rightarrow 5)$ linked.

fragment ions, which suggests that both LAM contain very few $\alpha(1 \rightarrow 2)$, $\alpha(1 \rightarrow 5)$ linkages.

This methodology will be used to identify the composition and linkages of LAMs from various mutant strains of both *M. tuberculosis* and *M. smegmatis*. Additionally, characterization of LAMs from both mutant and wild type strains after challenge with nonlethal doses of antibiotics as well as investigation of the larger oligomers (4–9 monosaccharide units) by using MS^n coupled with hydrolysis and enzymatic digestion procedures are currently underway.

Conclusions

We have applied electrospray mass spectrometric methods for the structural analysis of lipoarabinomannans obtained from the cell wall of *M. tuberculosis* and *M. smegmatis*. Mild acid hydrolysis experiments, utilizing as little as 10 μg of LAM, were used to facilitate MS characterization of small segments of the LAM. By using FT-ICRMS and exact mass measurements, we have unambiguously identified a series of arabinose oligomers from both *M. smegmatis* and *M. tuberculosis*, while mono-, di-, and trimannose capping motifs were only observed in *M. tuberculosis* LAM. From the relative abundance of the Man_mAra_n species (m = 1–3, n = 1–3) the ratio of the mono-, di-, and trimannose caps has been determined to be 1.00:9.00:1.15, respectively. CID of lithiated arabinose trimer standards yielded ions that could be used to differentiate between arabinose trimers that are $\alpha(1 \rightarrow 2)$,$\alpha(1 \rightarrow 5)$ and $\alpha(1 \rightarrow 5)$,$\alpha(1 \rightarrow 5)$ linked. Comparison of product ions in the MS^3 spectra of the arabinose trimers from *M. smegmatis* and *M. tuberculosis* confirmed that they are predominantly $\alpha(1 \rightarrow 5)$,$\alpha(1 \rightarrow 5)$ linked. Future work will entail determination of the linkage of larger arabinose oligosaccharides as well as the analogous Ara-Man oligomers.

Acknowledgments

JAL, LHS, and CJP gratefully acknowledge the National Institutes of Health (grant no. GM 47356) for financial support of this work. The authors thank Professor Todd L. Lowary of the University of British Columbia for generously providing arabinose trimer standards.

References

1. Bloom, B. R.; Murray, C. J. L. Tuberculosis—Commentary on a Reemergent Killer. *Science* **1992,** *257*, 1055–1064.
2. Chatterjee, D. The Mycobacterial Cell Wall: Structure, Biosynthesis, and Sites of Drug Action. *Curr. Opin. Chem. Biol.* **1997,** *1*, 579–588.
3. Brennan, P. J.; Nikaido, H. The Envelope of Mycobacteria. *Annu. Rev. Biochem.* **1995,** *64*, 29–63.
4. Nigou, M.; Gilleron, M.; Puzo, G. Lipoarabinomannans: From Structure to Biosynthesis. *Biochimie* **2003**, *85*, 153–166
5. Khoo, K. H.; Dell, A.; Morris, H. R.; Brennan, P. J.; Chatterjee, D. Inositol Phosphate Capping of the Nonreducing Termini of Lipoarabinomannan from Rapidly Growing Strains of Mycobacterium. *J. Biol. Chem.* **1995,** *270*, 12380–12389.
6. Treumann, A.; Feng, X.; McDonnell, L.; Derrick, P.; Ashcroft, A.; Chatterjee, D.; Homans, S. 5-Methylthiopentose: A New Substituent on Lipoarabinomannan in *Mycobacterium tuberculosis*. *J. Mol. Biol.* **2002,** *316*, 89–100.
7. Chan, J.; Fan, X.; Hunter, S. W.; Brennan, P. J.; Bloom, B. R. Lipoarabinomannan, a Possible Virulence Factor Involved in Persistence of *Mycobacterium tuberculosis* within Macrophages. *Infect. Immun.* **1991,** *59*, 1755–1761.
8. Chatterjee, D.; Khoo, K. H. Mycobacterial Lipoarabinomannan: An Extraordinary Lipoheteroglycan with Profound Physiological Effects. *Glycobiology* **1998,** *8*, 113–120.
9. Chatterjee, D.; Roberts, A. D.; Lowell, K.; Brennan, P. J.; Orme, I. M. Structural Basis of Capacity of Lipoarabinomannan to Induce Secretion of Tumor-Necrosis Factor. *Infect. Immun.* **1992,** *60*, 1249–1253.
10. Nigou, J.; Gilleron, M.; Rojas, M.; Garcia, L. F.; Thurnher, M.; Puzo, G. Mycobacterial Lipoarabinomannans: Modulators of Dendritic Cell Function and the Apoptotic Response. *Microbes Infect.* **2002,** *4*, 945–953.
11. Schlesinger, L. S.; Hull, S. R.; Kaufman, T. M. Binding of the Terminal Mannosyl Units of Lipoarabinomannan from a Virulent-Strain of *Mycobacterium tuberculosis* to Human Macrophages. *J. Immunol.* **1994,** *152*, 4070–4079.
12. Strohmeier, G. R.; Fenton, M. J. Roles of Lipoarabinomannan in the Pathogenesis of Tuberculosis. *Microbes Infect.* **1999,** *1*, 709–717.
13. Venisse, A.; Fournie, J. J.; Puzo, G. Mannosylated Lipoarabinomannan Interacts with Phagocytes. *Eur. J. Biochem.* **1995**, *231*, 440–447.
14. Sidobre, S.; Nigou, J.; Puzo, G.; Riviere, M. Lipoglycans are Putative Ligands for the Human Pulmonary Surfactant Protein A Attachment to Mycobacteria—Critical Role of the Lipids for Lectin-Carbohydrate Recognition. *J. Biol. Chem.* **2000,** *275*, 2415–2422.
15. Sieling, P. A.; Chatterjee, D.; Porcelli, S. A.; Prigozy, T. I.; Mazzaccaro, R. J.; Soriano, T.; Bloom, B. R.; Brenner, M. B.; Kronenberg, M.; Brennan, P. J.; Modlin, R. L. Cd1-Restricted T-Cell Recognition of Microbial Lipoglycan Antigens. *Science* **1995,** *269*, 227–230.
16. Venisse, A.; Berjeaud, J. M.; Chaurand, P.; Gilleron, M.; Puzo, G. Structural Features of Lipoarabinomannan from *Mycobacterium bovis* BCG—Determination of Molecular-Mass by Laser-Desorption Mass-Spectrometry. *J. Biol. Chem.* **1993,** *268*, 12401–12411.
17. Ludwiczak, P.; Brando, T.; Monsarrat, B.; Puzo, G. Structural Characterization of *Mycobacterium tuberculosis* Lipoarabinomannans by the Combination of Capillary Electrophoresis and Matrix-Assisted Laser Desorption/Ionization Time-of-Flight Mass Spectrometry. *Anal. Chem.* **2001,** *73*, 2323–2330.
18. Monsarrat, B.; Brando, T.; Condouret, P.; Nigou, J.; Puzo, G. Characterization of Mannooligosaccharide Caps in Mycobacterial Lipoarabinomannan by Capillary Electrophoresis/Electrospray Mass Spectrometry. *Glycobiology* **1999,** *9*, 335–342.
19. Cancilla, M. T.; Gaucher, S. P.; Desaire, H.; Leary, J. A. Combined Partial Acid Hydrolysis and Electrospray Ionization-Mass Spectrometry for the Structural Determination of Oligosaccharides. *Anal. Chem.* **2000,** *72*, 2901–2907.
20. Desaire, H.; Leary, J. A. Differentiation of Diastereomeric *N*-Acetylhexosamine Monosaccharides Using Ion Trap Tandem Mass Spectrometry. *Anal. Chem.* **1999,** *71*, 1997–2002.
21. Gaucher, S. P.; Leary, J. A. Stereochemical Differentiation of Mannose, Glucose, Galactose, and Talose Using Zinc(II) Diethylenetriamine and ESI-Ion Trap Mass Spectrometry. *Anal. Chem.* **1998,** *70*, 3009–3014.
22. Leavell, M. D.; Leary, J. A. Stabilization and Linkage Analysis of Metal-Ligated Sialic Acid Containing Oligosaccharides. *J. Am. Soc. Mass Spectrom.* **2001,** *12*, 528–536.

23. Desaire, H.; Leary, J. Utilization of MS3 Spectra for the Multicomponent Quantification of Diastereomeric *N*-Acetylhexosamines. *J. Am. Soc. Mass Spectrom.* **2000,** *11*, 1086–1094.
24. Chatterjee, D.; Lowell, K.; Rivoire, B.; McNeil, M. R.; Brennan, P. J. Lipoarabinomannan of *Mycobacterium tuberculosis*—Capping with Mannosyl Residues in Some Strains. *J. Biol. Chem.* **1992,** *267*, 6234–6239.
25. Khoo, H.; Tang, J.; Chatterjee, D. Variation in Mannose-Capped Terminal Arabinan Motifs of Lipoarabinomannans from Clinical Isolates of *Mycobacterium tuberculosis* and *Mycobacterium avium* Complex. *J. Biol. Chem.* **2001,** *276*, 3863–3871.
26. Asam, M. R.; Glish, G. L. Tandem Mass Spectrometry of Alkali Cationized Polysaccharides in a Quadrupole Ion Trap. *J. Am. Soc. Mass Spectrom.* **1997,** *8*, 987–995.
27. Hofmeister, G. E.; Zhou, Z.; Leary, J. A. Linkage Position Determination in Lithium-Cationized Disaccharides—Tandem Mass Spectrometry and Semiempirical Calculations. *J. Am. Chem. Soc.* **1991,** *113*, 5964–5970.
28. Smith, G.; Leary, J. Mechanistic Studies of Diastereomeric Nickel(II) *N*-Glycoside Complexes Using Tandem Mass Spectrometry. *J. Am. Chem. Soc.* **1998,** *120*, 13046–13056.
29. Smith, G.; Leary, J. Differentiation of Stereochemistry of Glycosidic Bond Configuration: Tandem Mass Spectrometry of Diastereomeric Cobalt-Glucosyl-Glucose Disaccharide Complexes. *J. Am. Soc. Mass Spectrom.* **1996,** *7*, 953–957.
30. Smith, G.; Pedersen, S.; Leary, J. Stereoselective β-Hydrogen Elimination from Nickel(II)-*N*-Glycoside Complexes. *J. Org. Chem.* **1997,** *62*, 2152–2154.
31. Staempfli, A.; Zhou, Z. R.; Leary, J. A. Gas-Phase Dissociation Mechanisms of Dilithiated Disaccharides—Tandem Mass Spectrometry and Semiempirical Calculations. *J. Org. Chem.* **1992,** *57*, 3590–3594.
32. Zhou, Z. R.; Ogden, S.; Leary, J. A. Linkage Position Determination in Oligosaccharides—MS/MS Study of Lithium-Cationized Carbohydrates. *J. Org. Chem.* **1990,** *55*, 5444–5446.
33. Gaucher, S.; Cancilla, M.; Phillips, N.; Gibson, B.; Leary, J. Mass Spectral Characterization of Lipooligosaccharides from *Haemophilus influenzae* 2019. *Biochemistry* **2000,** *39*, 12406–12414.
34. Domon, B.; Costello, C. E. A Systematic Nomenclature for Carbohydrate Fragmentations in FAB-MS MS Spectra of Glycoconjugates. *Glycoconj. J.* **1988,** *5*, 397–409.